Numerical Study of Crystal Sedimentation Induced Segregation Band in Steel Ingots

M. Wu[1,2], A. Kharicha[1,2] and A. Ludwig[2]

[1] Christian Doppler Laboratory for Advanced Process Simulation of Solidification and Melting,
[2] Chair of Simulation and Modelling of Metallurgical Processes, Montanuniversitaet Leoben, Franz-Josef Str. 18, Leoben, Austria.

Abstract

A discussion on the crystal sedimentation induced segregation band in steel ingots is made. It refers to a positive segregation zone as located in the columnar or branched columnar crystal structure region, just near and slightly above the columnar-to-equiaxed transition (CET), following the locus of the CET, starting from the bottom corner and extending upwards into the middle radius region. It was traditionally classified as A-segregates or A-shape channel segregation, due to the appearance of A-shape. The recent numerical study, however, shows that it forms with a different mechanism from the mostly observed A-segregates in the upper middle-radius region. Many previous studies, both laboratory experiment and numerical modelling, have verified that the middle-radius A-segregates in the pure columnar or branched columnar structure region originated from the mush destabilization due to the flow. The new modelling result shows that an A-shape segregation band adjacent to CET can form by the motion of equiaxed crystals, and their interaction with the growing columnar dendrite tips near the junction of the columnar dendrites and the piles of the equiaxed crystals. We infer that this segregation band might provide a favoured location for the initiation of A-segregates in the middle-radius region of the upper part steel ingot.

Keywords: Ingot, Macrosegregation, Sedimentation, Solidification, Numerical model.

1. Introduction

Different types of macrosegregation were observed in steel ingots. One of them was described as "rope-like" A-segregates by Blank and Pickering from a 15-ton steel ingot [1], or termed as "streak-type" inverted-V segregation by Ohno from a laboratory NH_4Cl-Water experiment [2]. They were typically found near the columnar to equiaxed transition (CET), following the locus of CET, starting from the bottom corner and extending upwards into the mid-radius region of the ingot Fig. 1 (a). Tentative explanation to this segregation by the original authors was that the solute-enriched melt was entrapped in the gap between the sideways-growing columnar dendrites and the pile of sedimentation-induced equiaxed dendrites, as shown in Fig. 1(b) [1, 3]; or that the settling of crystals in the lower part of the crystal-liquid mixture resulted in tears at the position of CET and those tears were filled by the solute-enriched melt [2]. Additional experimental facts [4-5] seemed to confirm that this kind of segregation is somehow related to the crystal sedimentation. Therefore, we term it here as "sedimentation induced segregation band".

This kind of segregation was later on classified into A-segregates or A-shape channel segregation, probably due to its similar appearance of A-shape as mostly observed A-segregates in middle-radius region of the ingot. The definition of A-segregates according to their appearance leads to confusion. Many researchers don't distinguish this kind of segregation band from the general term of A-segregates. It has been verified that the middle-radius A-segregates or channel segregation can originate from the mush destabilization by interdendritic thermo-solutal convection in the stationary columnar dendrite region [6-12]. The role of equiaxed sedimentation in the formation of segregation band adjacent to CET was underestimated.

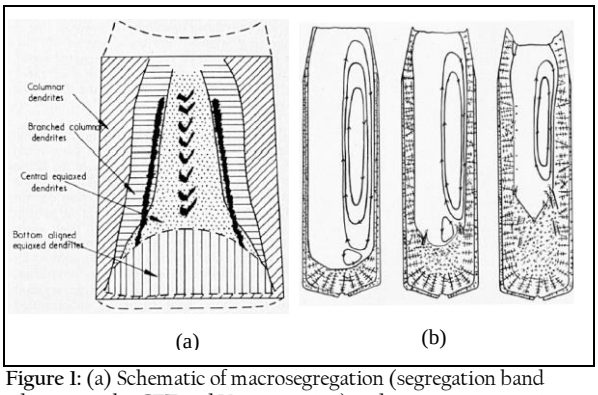

Figure 1: (a) Schematic of macrosegregation (segregation band adjacent to the CET and V-segregation) and as-cast structure in a 15-ton steel ingot [1]; (b) explanation to the segregation band by the solidification sequence and the liquid flow and crystal sedimentation pattern [3].

The mush destabilization theory fails to explain the sedimentation induced segregation band. Therefore, a modelling study is here performed for this purpose.

2. Numerical study

2.1 The numerical model in brief

A multiphase solidification model was proposed by the current authors for modelling the macrosegregation in steel ingots, with consideration of the mixed columnar-equiaxed structure [13-14]. It was recently extended to consider the effect of shrinkage cavity formation [15]. The striking feature of the model is that four phases are considered: the liquid melt, the solidifying solid with columnar morphology, the solidifying solid with equiaxed morphology, and the gas phase (or covering liquid slag). With consideration of the above phases and their interactions, it is possible to investigate the sedimentation induced macrosegregation with following necessary information: the progress of columnar tip front and growth of columnar tree trunks, the nucleation and growth of equiaxed grains, the melt flow and equiaxed crystal sedimentation, the solute partitioning at the solid/liquid interface, the transport of the solute species, the shrinkage cavity and its effect on the macrosegregation, the interaction or competition between growing columnar and equiaxed phases and the occurrence of columnar to equiaxed transition (CET).

2.2 Numerical simulation of a 10-ton steel ingot

A 10-ton ingot, historically cast for analysis of macrosegregation [16], was recently simulated with the four-phase solidification model. The ingot had an octagonal cross-section. A multicomponent alloy is cast, but it is here simplified as a binary alloy of Fe-0.3wt.%C. No mould filling is calculated, and the mould is assumed to be initially filled with liquid melt of 1782 K (above the liquidus 1781.02 K). As solidification starts, the casting shrinks and it sucks the liquid covering slag phase from the top 'pressure inlet' to feed the solidification shrinkage. A heterogeneous nucleation law was implemented to mimic the origin of equiaxed crystals by different mechanisms. Nucleation parameters are: n_{max} = 5.0 x 10^{-9} m^{-3}, ΔT_N = 5.0 K, ΔT_σ = 2.0 K. The material properties, boundary conditions and other parameters as used for the simulation were presented previously [15]. A concept of "equiaxed grain envelope" is employed to treat the equiaxed dendritic morphology. A certain amount of solid 'dendrite' inside the grain envelope (f_{si} = 0.6) is assumed, and it is further calibrated with experiment.

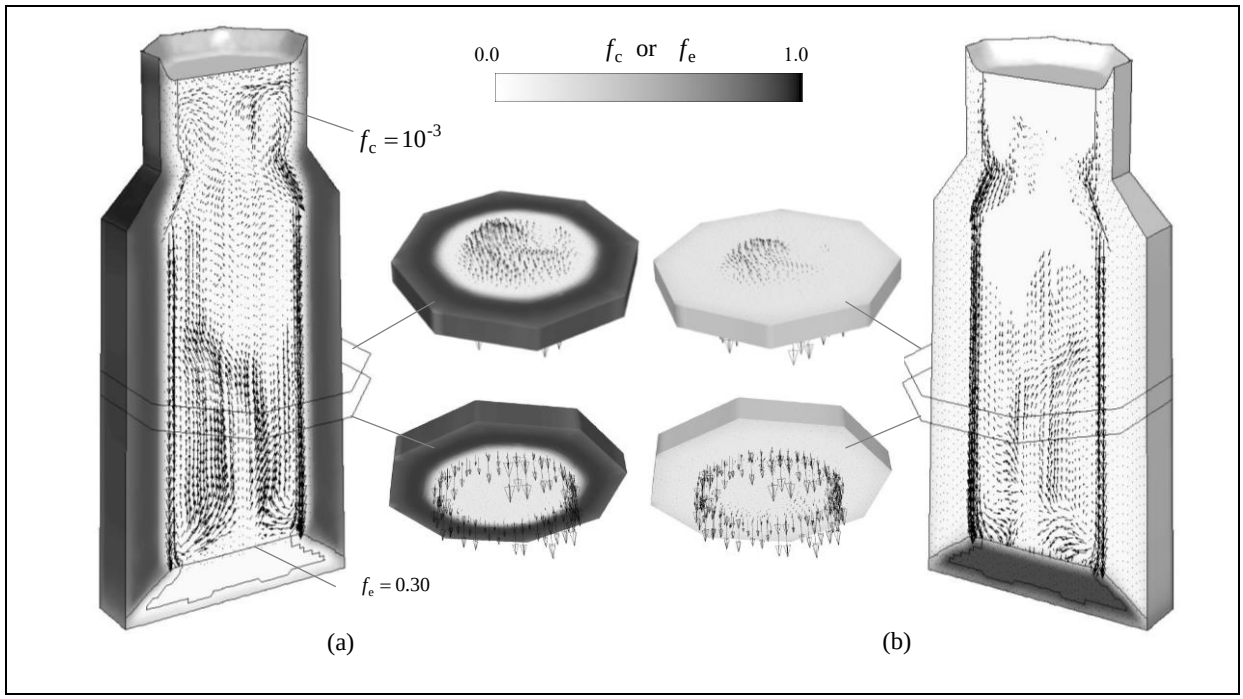

Figure 2: Solidification sequence at 1880 s. Both columnar and equiaxed volume fraction, f_c and f_e, in the centre vertical section are shown in grey scale. (a) The velocity of the melt, $\vec{u}_\ell$ is shown together with f_c, while (b) the velocity of the equiaxed crystals, $\vec{u}_e$ is with f_e. Additionally, the phase distributions and velocity fields in 2 horizontal segments are also shown.

The solidification sequence at 1880 s is shown in Fig. 2. The cooling and solidification start from the mould wall. Columnar phase develops from outer surface and grows towards casting centre. Equiaxed grains originate and grow in the front of columnar tips, and those equiaxed grains sink and try to settle in the bottom region. The melt is dragged downwards along the columnar tip front by the sinking equiaxed grains, which in turn induces a rising flow in the centre. Thermal-solutal buoyancy contributes to the flow as well, both in the interdendritic region and in the bulk. Both $\vec{u}_\ell$ and $\vec{u}_e$ fields are not stable. Sedimentation of crystals in the bottom causes the volume fraction of the equiaxed phase to reach a quite high level. As f_e in the lower part is high enough to block the growth of columnar tips, the columnar-to-equiaxed transition (CET) occurs. In the upper part of the ingot, the columnar

tips can continue to grow, as no sufficient equiaxed crystals exist in the front of them. The flow and crystal sedimentation are key mechanisms for the formation of macrosegregation in the ingot casting. The final segregation result is shown in Fig. 3. A large positive segregation area just below the top shrinkage cavity is predicted. A conic negative segregation zone is found in the bottom region, which coincides with the equiaxed sedimentation zone.

As shown in Fig. 3 (a), a positive A-shape segregation band starts from the bottom corners, develops slightly above the packed equiaxed zone, and extends to the upper part of the ingot. This numerically-predicted A-shape segregation band agrees nicely with the lower part 'sedimentation induced segregation band' of the experiment (Fig. 3(b)). Experimentally, many fine channels of A-segregates were also observed in the upper part and near the middle-radius region, but the numerical result shows only some dispersed positive segregation (no clear channels) in the vertical section. With finer gray scale, we do predict a strong tendency of developing channel segregation (horizontal section) in the upper middle-radius region. The grid size for the current simulation (~18 mm) is too coarse to calculate fine channels.

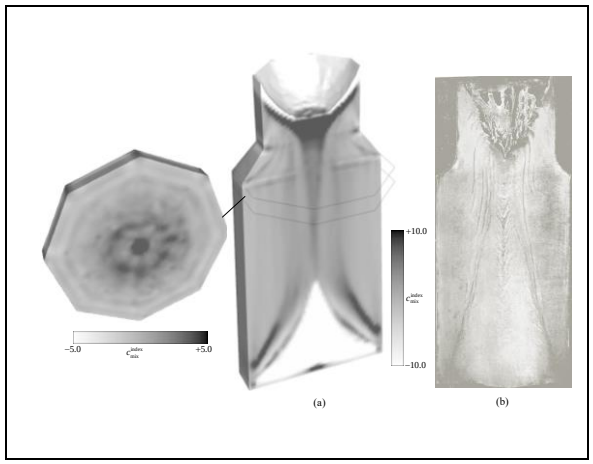

Figure 3: (a) Numerically predicted segregation and (b) comparison with experiment, Sulphur print.

2.3 Sedimentation induced segregation band

Formation of macrosegregation can be analyzed by the variation of the local mixture concentration c_{mix} in response to different transport quantities. With an approximation of $\bar{\rho} \approx \rho_\ell \approx \rho_{\mathrm{e}} \approx \rho_{\mathrm{c}}$, the variation of c_{mix} depends on three terms:

$$\frac{\partial}{\partial t} c_{\mathrm{mix}} = (c_\ell - c_{\mathrm{e}}) \nabla \cdot (f_{\mathrm{e}} \vec{u}_{\mathrm{e}}) - f_\ell \vec{u}_\ell \cdot \nabla c_\ell - f_{\mathrm{e}} \vec{u}_{\mathrm{e}} \cdot \nabla c_{\mathrm{e}} . \qquad (1)$$

These three terms correspond to three macrosegregation mechanisms during mixed columnar-equiaxed solidification. The first term $(c_\ell - c_{\mathrm{e}}) \nabla \cdot (f_{\mathrm{e}} \vec{u}_{\mathrm{e}})$ represents the contribution of the accumulation or depletion of equiaxed phase. $(c_\ell - c_{\mathrm{e}})$ has usually a positive value for the alloy element with its partition coefficient k less than one. A positive value of $\nabla \cdot (f_{\mathrm{e}} \vec{u}_{\mathrm{e}})$, i.e. the depletion of equiaxed phase (Fig. 4 I-(a)) or to say more equiaxed phase leaves than enters the reference volume element, leads to increase of c_{mix}, developing positive segregation. In the opposite, a negative value of $\nabla \cdot (f_{\mathrm{e}} \vec{u}_{\mathrm{e}})$, i.e. accumulation of equiaxed phase (Fig. 4 II-(a)), would lead to a decrease of c_{mix}, i.e. developing negative segregation. The second term $-f_\ell \vec{u}_\ell \cdot \nabla c_\ell$ represents the contribution of the interdendritic melt flow through the stationary mushy zone (columnar dendrite region or packed equiaxed network) to the formation of macrosegregation. A positive value of the term $-f_\ell \vec{u}_\ell \cdot \nabla c_\ell$, i.e. the melt flows in the direction against the direction of ∇c_ℓ, leads to the formation of positive segregation (Fig. 4 I-(b)). A negative value of the term $-f_\ell \vec{u}_\ell \cdot \nabla c_\ell$, i.e. the melt flows in the same direction of ∇c_ℓ, leads to the formation of negative segregation (Fig. 4 II-(b)). The third term $-f_{\mathrm{e}} \vec{u}_{\mathrm{e}} \cdot \nabla c_{\mathrm{e}}$ describes the transport of equiaxed phase, which has a concentration gradient ∇c_{e} (equiaxed crystals entering the volume element have different concentration from those leaving the volume element). According to previous study, the contribution of this term is negligible [15].

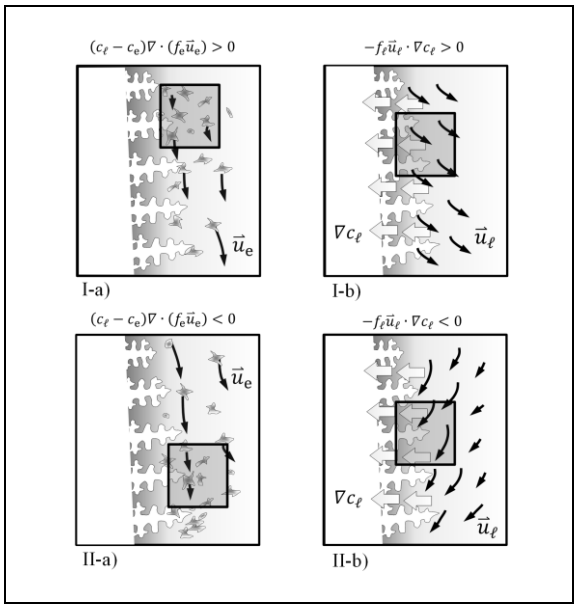

Figure 4: Schematic of macrosegregation mechanisms during mixed columnar-equiaxed solidification.

The above theory is applied to study the A-shape segregation band in the lower part of the ingot. The evolution sequence of $c_{\mathrm{mix}}^{\mathrm{index}}$, $\partial c_{\mathrm{mix}}/\partial t$, and the other three contributing terms of Eq. (1) is shown in Fig. 5. The A-shape segregation band (Fig. 5 (a)-(b)) develops in the columnar structure region between isolines of $f_{\mathrm{c}} = 10^{-3}$ and 0.5, some distance above the bottom equiaxed packing border, as shown with the dark mark (as pointed by white arrow) of the term $\partial c_{\mathrm{mix}}/\partial t$ in Fig. 5 (c). This dark mark is the outcome of the competition between the first and the second terms, as seen in Fig. 5 (d) of another dark mark and in Fig. 5 (e) of the bright mark. The contribution of the third term is negligible, Fig. 5(f). Actually, the dark mark of $\partial c_{\mathrm{mix}}/\partial t$ in Fig. 5 (c) comes from the balance of $(c_\ell - c_{\mathrm{e}}) \nabla \cdot (f_{\mathrm{e}} \vec{u}_{\mathrm{e}})$ and $-f_\ell \vec{u}_\ell \cdot \nabla c_\ell$, but the term $(c_\ell - c_{\mathrm{e}}) \nabla \cdot (f_{\mathrm{e}} \vec{u}_{\mathrm{e}})$ overwhelms the term of $-f_\ell \vec{u}_\ell \cdot \nabla c_\ell$. A positive value of $(c_\ell - c_{\mathrm{e}}) \nabla \cdot (f_{\mathrm{e}} \vec{u}_{\mathrm{e}})$, dark mark in Fig. 5 (d), means that the depletion of the equiaxed phase locally, and the space of the leaving equiaxed phase is compensated by the solute-enriched liquid melt. This effect may be difficult to observe from the velocity fields, as the variations of the melt flow and the velocity of equiaxed phase are quite small. The

above analysis suggests that the formation of the A-shape segregation band is related to the motion of equiaxed phase: some equiaxed crystals leave or the motion of the equiaxed crystals accelerates at a certain region.

It seems clear that the A-shape segregation band is not the same type of A-segregates in the middle-radius region. Firstly, they appear differently: the former is thick positively segregation region, which starts from the ingot bottom corner and tends to appear in the form of a truncated hollow cone in parallel to the locus of the columnar-to-equiaxed transition, while the latter includes many thin and curved channels (maybe laminar structure) of segregation and they are located in the middle-radius columnar structure region. Secondly, they are caused by different mechanisms: the former is caused by the motion of equiaxed phase, while the latter is caused by the mush destabilization due to the melt flow at the columnar tip front and by the flow-solidification interaction in the mushy zone [6-12, 17-18].

The early explanation (Fig. 1(b)) of Blank and Pickering [1] and that of Ohno [2] to the crystal sedimentation induced segregation band, called as "rope-like" A-segregates or "steak-type" inverted V-segregation whatever, are not exactly the same as what we found in Fig. 5, but the early works [1-2] provided valuable clues that the formation of the A-shape segregation band is related to the motion and sedimentation of equiaxed crystals.

Another fact (Fig. 3(b)) is that some middle radius A-segregates (thin channels) are simply the extension of the sedimentation induced A-shape segregation band. This is also observed in many other ingots [1, 16]. It means that the crystal sedimentation induced A-shape segregation band presents a source of the A-segregates, or provides a favorite position to initialize the A-segregates in the middle radius region of the ingot. We still believe that most A-segregates in the middle radius region of the ingot originate from the mush destabilization in the columnar zone due to the thermo-solutal convection, but the sedimentation-induced A-shape segregation band might provide a favored location for the mush destabilization in the vicinity of the columnar tip front.

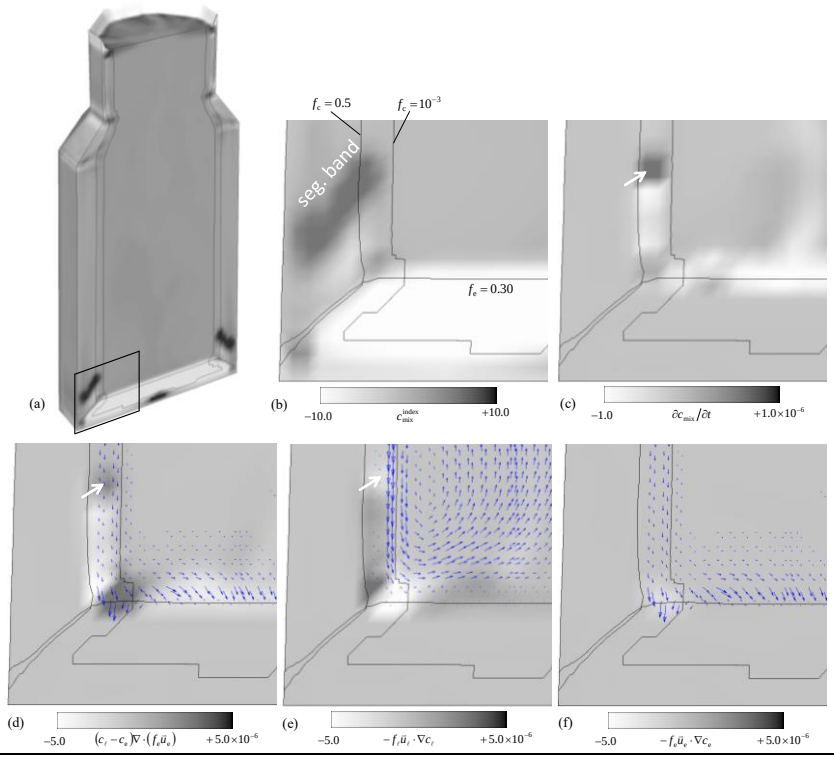

Figure 5: Analysis of A-shape segregation band for the moment at 1080 s. a) Map of segregation index $c_{\mathrm{mix}}^{\mathrm{index}} = 100 \times (c_{\mathrm{mix}} - c_0)/c_0$; b) zoomed segregation map near the corner; c) the variation of the mixture concentration $\partial c_{\mathrm{mix}}/\partial t$; d) map of the term $(c_\ell - c_e)\nabla \cdot (f_e \vec{u}_e)$ overlaid with vectors of the equiaxed velocity; e) map of the term $-f_\ell \vec{u}_\ell \cdot \nabla c_\ell$ overlaid with vectors of the melt velocity; f) map of the term $-f_e \vec{u}_e \cdot \nabla c_e$ overlaid with vectors of the equiaxed velocity. Three isolines of phase fraction ($f_c = 10^{-3}$, 0.5 and $f_e = 0.30$) are also shown to indicate different phase regions.

4. Conclusion

The numerical study shows that an A-shape segregation band adjacent to CET can form due to the motion of equiaxed crystals, and their interaction with the growing columnar dendrite tips near the junction of the columnar dendrites and the piles of the equiaxed crystals. This segregation band might provide a favoured location for the initiation of A-segregates in the middle-radius region of the upper part steel ingot.

References

1. J.R. Blank, F.B. Pickering, Proc. of 1st SP conf. in 1967, UK, *The solidification of metals*, 1968:370.
2. Ohno, Proc. of 1st SP conf. in 1967, UK, *The solidification of metals*, 1968:349.
3. J.R. Blank, W. Johnson, *Steel Times*, July 23. 1965, p.110.
4. A. Kohn, Proc. of 1st SP conf. in 1967, UK, *The solidification of metals*, 1968:354.
5. K.W. Andrews, C.R. Gomer, Proc. of 1st SP conf. in 1967, UK, *The solidification of metals*, 1968:363.

6. R. J. McDonald, J.D. Hunt, *Trans. Metal. Society of AIME*, 1969, **245**: 1993.
7. K. Suzuki, T. Miyamoto, *Trans. ISIJ*, 1978, **18**: 80.
8. M.G. Worster, *Annu. Rev. Fluid Mech.*, 1997, **29**:91.
9. J.C. Ramirez, C. Beckermann, *Metall. Mater. Trans. A*, 2003, **34A**:1525.
10. M. Zaloznik, H. Combeau, *Int. J. Thermal Sci.*, 2010, **49**: 1500.
11. J. Li, M. Wu, J. Hao, A. Ludwig, *Comp. Mater. Sci.*, 2012, **55**:407.
12. L. Yuan, P.D. Lee, *Acta Mater.*, 2012, **60**:4917.
13. M. Wu, A. Ludwig, *Metall. Mater. Trans. A*, 2006, **37A**:1613.
14. M. Wu, A. Ludwig, *Metall. Mater. Trans. A*, 2007, **38A**:1465.
15. M. Wu, A. Ludwig, A. Kharicha, *Applied Math. Modell.*, 2017, **41**:102.
16. Report on the heterogeneity of steel ingots, *J. Iron Steel Inst.*, 1926, **103**:39.
17. M. Wu, J. Li, A. Kharicha, A. Ludwig, *Comp. Mater. Sci.*, 2013, **79**:830.
18. M. Wu, J. Li, A. Kharicha, A. Ludwig, *Comp. Mater. Sci.*, 2014, **92**:267